

Imaging and Clinical Features of Thyroid Cancer in Children and Adolescents¹

소아와 청소년에서 갑상선암의 영상의학적 소견과 임상적 특징¹

Kang Young Lee, MD¹, Hyun Sook Hong, MD¹, Eun Hye Lee, MD¹, Beom-Ha Yi, MD¹,
Hae Kyung Lee, MD¹, Yong-Wha Lee, MD², Eun Suk Koh, MD³

Departments of ¹Radiology, ²Laboratory Medicine and Genetics, ³Pathology, Soonchunhyang University College of Medicine, Bucheon Hospital, Bucheon, Korea

Purpose: To evaluate clinical and imaging features of pediatric thyroid cancer, including BRAF^{V600E} mutation status in papillary thyroid cancer (PTC).

Materials and Methods: We evaluated clinical findings including BRAF^{V600E} status, ultrasound (US), and CT features of 13 pediatric patients with thyroid cancer. US findings were retrospectively analyzed for location, presence of a nodule, echotexture, echogenicity, calcifications, margin, shape, intranodular vascularity and abnormal lymph nodes. CT characteristics of the lesions, including attenuation, calcification, and measured degree of enhancement, were assessed.

Results: The patients included three boys and ten girls with a mean age of 15.5 years (range 6-18 years). No patient was exposed to radiation. Palpable neck mass was the most common presentation. Eleven of 13 patients (84.6%) were diagnosed with PTC, and two (15.4%) had follicular thyroid cancer (FTC). Nine of 13 (69.2%) had high T-staging. BRAF^{V600E} mutations were detected in 30.0% of PTC patients. A diffusely enlarged thyroid with calcifications ($n = 2$) or nodules ($n = 7$) was detected on US. All PTC nodules showed malignant US findings and one FTC displayed an indeterminate nodule. Nodules generally showed low attenuation on enhanced CT ($n = 11/12$).

Conclusion: US demonstrated enlarged glands with calcifications or nodules. Diffusely enlarged thyroids with microcalcifications should be evaluated using fine-needle aspiration. A low attenuation nodule was a common finding on enhanced CT.

Index terms

Thyroid Neoplasms
Child
Ultrasonography
Tomography, X-Ray Computed
Proto-Oncogene Proteins B-Raf

Received November 15, 2010; Accepted May 23, 2011

Corresponding author: Hyun Sook Hong, MD
Department of Radiology, Soonchunhyang University
Bucheon Hospital, 1174 Jung-dong, Wonmi-gu,
Bucheon 420-767, Korea.
Tel. 82-32-621-5851 Fax. 82-32-621-5874
E-mail: hshong@schbc.ac.kr

Copyrights © 2011 The Korean Society of Radiology

INTRODUCTION

The incidence of thyroid nodules in children and adolescents is estimated to be between 1% and 2% (1). However, because of the detection of incidental and subclinical thyroid nodules using diagnostic imaging modalities, this incidence may be increasing. The risk of malignancy of thyroid nodules in children ranges between 14 to 40%, which is much higher than that of adults (2). The estimated annual incidence of primary thyroid carcinoma in this population worldwide is 0.5-10 cases per million (2). In Korea, thyroid cancer is the 11th most commonly diagnosed cancer in children under fourteen years old and the 10th most common cancer in girls ([http://](http://www.ncc.re.kr)

www.ncc.re.kr) (3).

In children, thyroid cancer tends to present at a more advanced stage than in adults, with a higher frequency of lymph node and pulmonary metastases (4). Distant metastasis is much less common than regional lymph node involvement, with the lung being the most common site of distant metastasis (5, 6).

Several reports have suggested that papillary thyroid carcinomas (PTCs) follow a more favorable course in young patients (< 21 years of age) (7). The reasons for this variation between children and adults are unknown, but are generally thought to be due to differences in mutations and oncogene expression in the thyroid (8). PTC is frequently associated

with genetic alterations leading to the activation of the mitogen-activated protein kinase signaling pathway (9, 10). A BRAF^{V600E} mutation at nucleotide position 1799 is a transversion of a thymine to an adenine, resulting in the conversion of a valine to a glutamate. The BRAF^{V600E} mutation is intrinsically associated with increased progression and aggressiveness of PTC. The reported frequency of a specific BRAF^{V600E} mutation in a PTC series ranged from 36% to 65% (11). However, the prevalence of the BRAF^{V600E} mutation in PTC in Korea is much higher (70-83%) than that of Western countries (12). Moreover, compared to rearranged during transfection/Papillary Thyroid Carcinomas, the BRAF^{V600E} abnormality is a more common genetic alteration, occurring in half of sporadic PTCs (13).

Ultrasonography (US) is commonly used for the evaluation of thyroid nodules. However, US and CT reports regarding the identification and features of suspicious nodules in children have been limited (14, 15).

The purpose of the present study was to review the clinical and imaging features of pediatric thyroid cancer and the status of molecular markers for the BRAF^{V600E} mutation in PTC, as well as analyzing the US and CT scan features of histopathologically confirmed thyroid cancer.

MATERIALS AND METHODS

This study was approved by the institutional review board with a waiver of informed consent.

Patients

Thirteen patients under eighteen years of age with histopathologically confirmed thyroid cancer from April 2003 to November 2009 were enrolled in the present study.

Medical records and imaging features were reviewed. The data collected included gender, age at diagnosis, presenting symptoms, lymph node involvement, distant metastases, tumor node metastasis (TNM)/pathological TNM classification, type of surgery performed, histological type, and molecular marker for the BRAF^{V600E} mutation associated with PTC. The TNM staging adopted in the present study was the American Joint Committee on Cancer (AJCC) classification for thyroid cancer (2010) (16).

Imaging Techniques and Image Interpretation Ultrasonography, FNA, and BRAF^{V600E} Analysis

Nine of 13 patients underwent US examination using an IU22 US, HDI 5,000 with a 12 MHz linear array transducer (Philips Medical Systems, Bothell, WA, USA), and a LOGIQ 700 MR system with a 10 MHz linear array transducer (GE Healthcare, Milwaukee, WI, USA). US findings were analyzed for location, presence of a nodule, echotexture, echogenicity, calcifications, margin, shape, intranodular vascularity on color Doppler images and abnormal lymph nodes in the lateral neck. US findings were analyzed based on the "Guidelines for the Thyroid US" by the Thyroid Study Group, Korean Society of Neuro- and Head and Neck Radiology (17). Nodule echogenicity was assessed according to the surrounding thyroid tissue and was classified as hyperechoic, isoechoic, hypoechoic, or markedly hypoechoic. The nodule echotexture was classified as homogeneous or heterogeneous. The margin of the nodule was classified as smooth or irregular. The shape of the nodule was categorized as either ovoid to round or taller than wide. The presence of calcifications and abnormal lymph nodes in the lateral neck was also recorded. Calcifications < 1 mm were classified as microcalcifications, and those > 1 mm were classified as macrocalcifications. Abnormal lymph node criteria included enlarged size (> 1.5 cm in the longest diameter at neck levels I and II, > 1.0 cm in the longest diameter at other neck node levels), spherical in shape (longitudinal/transverse diameter is < 1.5 cm), central necrosis, calcification, and chaotic vessels on a color Doppler image.

During color Doppler US examination, the presence of intranodular blood flow was evaluated for all lesions. A thyroid gland was considered to be goiterous when its volume exceeded the 97th percentile of the International Council for Control of Iodine Deficiency Disorders reference value (18).

BRAF^{V600E} mutations were analyzed in ten patients. A 22-gauge needle attached to a 10-mL disposable plastic syringe was used to perform ultrasound-guided fine needle aspiration biopsy. Each lesion was aspirated at least twice and the specimen for analysis of the BRAF^{V600E} mutation was obtained separately. The specimen was rinsed with 1 mL of normal saline, and then the wash-out was subjected to BRAF^{V600E} mutation analysis in three patients; another eight patients were evaluated for BRAF^{V600E} with samples from paraffin embedded

blocks. Dual-priming oligonucleotide-based multiplex polymerase chain reaction (PCR) amplification methods were used for the identification of mutations from a portion of the BRAF^{V600E} gene using Seeplex BRAF ACE Detection (Seegene, Inc., Seoul, Korea). Paraffin-embedded thyroid cancer tissue samples were examined twice, including DNA isolation and PCR amplification for the BRAF^{V600E} mutation (WH Lee).

Contrast-Enhanced Neck CT

Twelve of 13 patients underwent CT examination. A multi-detector row CT (MDCT) unit (Somatom Sensation 16; Siemens Medical Solutions, Erlangen, Germany) with 16 detector rows ($n = 4$); a spiral CT unit ($n = 6$) (HiSpeed Advantage; GE Healthcare, Milwaukee, WI, USA), and an MDCT unit with 64 detector rows ($n = 1$) (LightSpeed VCT; GE Healthcare, Milwaukee, WI, USA) were used. One patient underwent CT at an outside hospital. Typical contrast-enhanced CT imaging protocols for thyroid disease included unenhanced CT and contrast-enhanced CT images at 80 kVp and 60 mAs; field of view = 23 cm; collimation = 0.625 to 1.25 mm; and pitch = 0.9 to 1.3. Adaptation of the tube current corresponding to the body weight is used as a dose-saving CT protocol. For contrast-enhanced CT scans, 1.2-1.5 mL/kg of an iodinated contrast agent (Ultravist 360; Schering, Berlin, Germany), ranging from 0.3 to 3 mL/s, was injected, CT characteristics of the lesions, including attenuation, compared with the surrounding normal thyroid gland on pre- and post-contrast enhancement imaging, presence of calcifications, and measured degree of enhancement, were assessed. The degree of enhancement was calculated in Hounsfield units using the following formula: $[(\text{Density}_{\text{post}} - \text{Density}_{\text{pre}}) / \text{Density}_{\text{pre}}] \times 100\%$. The region of interest is positioned centrally with respect to the nodule or the goiterous enlarged lesions.

Eleven out of 13 patients underwent surgery; two patients were lost to follow up. All neoplastic lesions were staged according to the AJCC classification for thyroid cancer (2010) (16).

RESULTS

The series of patients consisted of ten girls and three boys, ranging in age 6 to 18 years old (mean, 15.5 years old). The clinical information is summarized in Table 1. No patient had

a history of radiation exposure. Eleven patients presented with a palpable neck mass, one patient presented with vocal cord palsy, and one patient presented with an incidentally detected thyroid mass on a chest CT scan, which was performed as a result of chest pain. The pathological diagnosis was confirmed at surgery ($n = 11$) or during fine needle aspiration biopsy ($n = 2$). Two patients who underwent hemithyroidectomy did not undergo preoperative US; one had nodular hyperplasia with intrathyroidal PTC, and the other had minimally invasive follicular thyroid cancer (FTC). Seven patients underwent a neck dissection due to metastatic lymphadenopathy. In total, eleven patients (84.6%) were diagnosed with PTC, of which all cases were of the classic type, and two patients (15.4%) were diagnosed with minimally invasive FTC. Metastasis was detected in nine patients; lymph node involvement was observed in eight (61.5%), and lung metastasis was detected in one (7.7%) BRAF^{V600E} mutations were detected in three (30.0%) of 10 PTC patients.

The US features of nine patients are summarized in Table 2. Seven patients had nodular lesions (Fig. 1) and the remaining two patients showed goiterous enlargement of the thyroid glands with microcalcifications (Fig. 2). All seven nodular lesions were solid and heterogeneous in echotexture. All six PTC nodules showed malignant US findings according to the "Guidelines for the Thyroid US" of the Thyroid Study Group, Korean Society of Neuro- and Head and Neck Radiology (17) [four findings ($n = 2$); three findings ($n = 1$); two findings ($n = 3$)]. One minimally invasive FTC demonstrated indeterminate nodule on US. The average nodule size had a maximum diameter of 1.93 cm (diameter range; 1.5-2.7 cm). Echogenicity of nodules was marked hypoechoic (3/7; 42.9%) (Fig. 1A), hypoechoic (1/7; 14.3%), isoechoic (2/7; 28.6%), or hyperechoic (1/7; 14.3%). Calcifications (micro- or macro-) were found in eight (88.9%) patients; the margin was irregular in six (85.7%) patients, all of which had PTC, and smooth in one patient with FTC. A taller than wide shape was found in two (28.6%) patients with PTC (Fig. 1A). All lesions revealed increased vascularity within the nodules or a goiterous enlarged gland on a color Doppler image. In two patients having diffuse enlargement with calcifications, the tumor replaced the entire gland. Abnormal neck lymph nodes were found in seven (77.8%) patients (Fig. 1B).

Table 1. Summary of Clinical Information in 13 Patients with Thyroid Cancer

No.	Sex	Age (year)	Pathology	Clinical Presentation	TNM Staging*	Type of Surgery	BRAF ^{V600E}	Type of Imaging Study
1	F	17	PTC	Vocal cord palsy	cT4a(s)N0Mx, stage I	FNA only	NT	US
2	F	6	PTC	Palpable neck mass	pT4a(m)N1bM1, stage II	TT, both MRND	-	US, CT
3	F	12	PTC, lymphocytic thyroiditis	Palpable neck mass	pT3(m)N1bM0, stage I	TT, CND, both MRND	-	US, CT
4	M	18	PTC	Incidental detection	pT3(s)N1bM0, stage I	TT, NR	-	US, CT
5	M	18	PTC	Incidental detection	pT3(s)N1bM0, stage I	TT, NR	-	US, CT
6	F	18	PTC	Palpable neck mass	pT2(s)N1bM0, stage I	TT, CND, Rt SND	+	US, CT
7	F	13	PTC	Palpable neck mass	pT4a(m)N1bM0, stage I	TT, CND, both ND	- (RET: -)	US, CT
8	F	12	PTC	Palpable neck mass	pT4a(m)N1bM0, stage I	TT, both FND	-	US, CT
9	M	17	PTC, nodular hyperplasia	Palpable neck mass	pT1a(s)N0M0, stage I	Left HT	-	CT
10	M	18	PTC	Palpable neck mass	cT3(s)N0M0, stage I	FNA only	-	CT
11	F	18	PTC	Palpable neck mass	pT3(s)N1bM0, stage I	TT, right ND	+	CT
12	F	17	FTC	Palpable neck mass	pT2(s)N0M0, stage I	TT	NT	US, CT
13	F	18	FTC	Palpable neck mass	pT2(s)N0M0, stage I	Left HT	NT	CT

Note.—*by the AJCC cancer staging manual and hand book, 7th Ed.

cTNM = clinical staging.

pTNM = pathological staging.

+ = mutation detected.

- = no mutation detected.

BRAF^{V600E} mutation = B type raf kinase, CND = central neck dissection, HT = hemithyroidectomy, FNA = fine needle aspiration, FND = functional neck dissection, FTC = follicular carcinoma, minimal invasive, MRND = modified radical neck dissection, ND = neck dissection, NR = node resection, NT = not taken, PTC = papillary carcinoma, RET oncogene = rearranged during transfection, SND = selective neck dissection, TNM = tumor node metastasis, TT = total thyroidectomy, US = ultrasonography

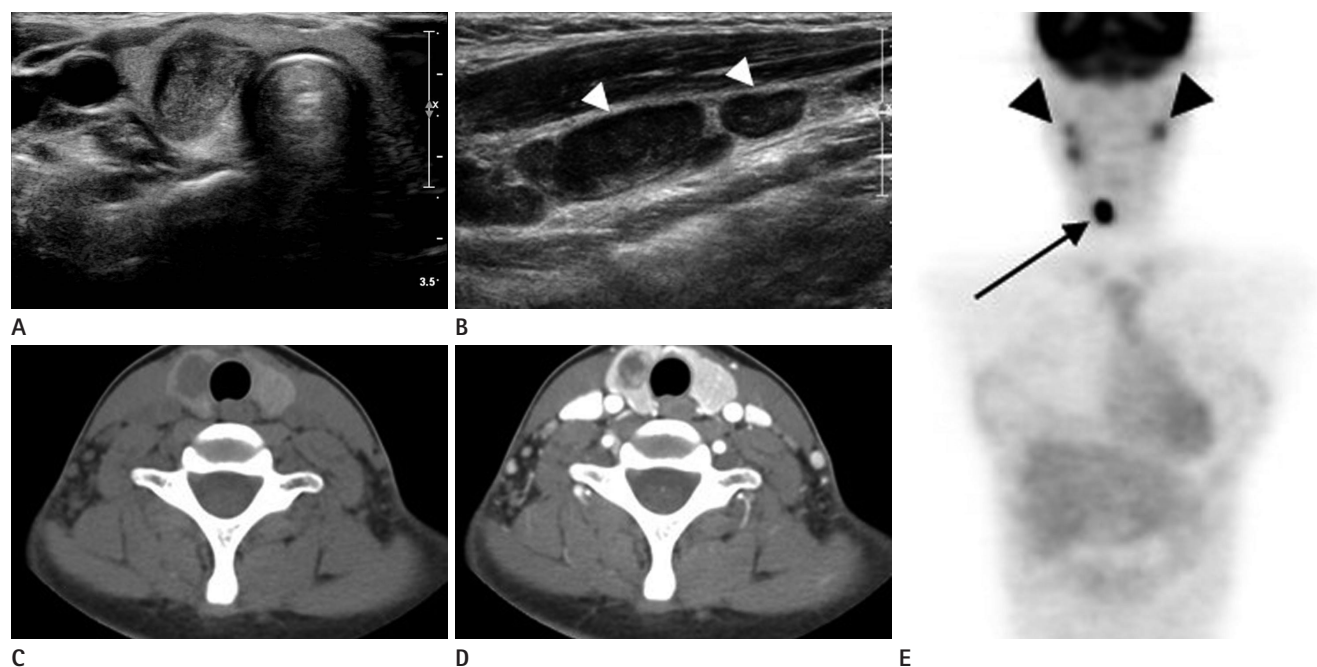


Fig. 1. An 18-year-old girl with papillary thyroid cancer presenting with a palpable neck mass. BRAF^{V600E} mutation analysis was positive. Transverse **(A)** gray-scale US images depict a typical malignant nodule with an irregular margin, marked hypoechogenicity with microcalcifications, and taller than wide shape with metastatic lymph nodes on the right at level III **(B)** (arrowheads).

The pre **(C)** and post contrast-enhanced **(D)** neck CT scan show a slightly enhancing low attenuated nodule of the right thyroid gland.

The PET-CT scan **(E)** demonstrates a hypermetabolic nodule in the right lobe p-SUV 8.9 (arrow) and lymph node metastases (arrowheads).

Histopathology of these lymph nodes show metastasis.

Note.—PET-CT = positron emission tomography-computed tomography

Twelve patients underwent CT examination. Among ten nodular lesions found, eight were low attenuation compared with the surrounding normal thyroid gland, and one had microcalcifications. The other two patients with underlying lymphocytic thyroiditis showed diffuse low attenuation on the pre-contrast scan, which was similar to that of the adjacent strap muscle and the nodular lesions were iso to low attenuation. The two remaining patients showed a goiterous enlarged gland with microcalcifications (Fig. 2). Eleven nodular lesions

showed low attenuation compared with well enhancing surrounding thyroid glands, which were detected more easily on post-contrast enhanced scans than on pre-contrast scans (Fig. 1C, D). The degree of enhancement ranged from 80% to 406% (mean: 166.9%) in 11 patients (one patient underwent a CT scan at an outside hospital; thus, the degree of enhancement could not be calculated). One nodule from the follicular thyroid cancer in our study was well enhanced (406%); the CT features are summarized in Table 3.

Table 2. Summary of Ultrasonographic Features in Nine Children and Adolescents with Thyroid Cancer

No.	Pathology	Lesion	Echotexture	Echogenicity	Calcifications	Margin	Shape	Vascularity	Abnormal LN
1	PTC	Nodule, Rt	Heterogenous	Marked hypoechoic solid	Micro	Irregular	Taller than wide	Increased	-
2	PTC	Nodule, Both	Heterogenous	Isoechoic solid	Micro and macro	Irregular	Ovoid to round	Increased	+: Bilateral, II-IV
3	PTC	Nodule, Lt	Heterogenous	Hyperechoic solid	Micro	Irregular	Ovoid to round	Increased	+: Lt, II-IV
4	PTC	Nodule, Lt	Heterogenous	Isoechoic solid	Micro	Irregular	Ovoid to round	Increased	+: Lt, II-IV
5	PTC	Nodule, Rt	Heterogenous	Marked hypoechoic solid	Micro and macro	Irregular	Ovoid to round	Increased	+: Rt, II-IV
6	PTC	Nodule, Rt	Heterogenous	Marked hypoechoic solid	Micro and macro	Irregular	Taller than wide	Increased	+: Rt, II-IV
7	PTC	Diffuse	Heterogeneous		Micro			Increased	+: Bilateral, II-IV
8	PTC	Diffuse	Heterogeneous		Micro			Increased	+: Bilateral, I-IV
9	FTC	Nodule, Rt	Heterogeneous	Slightly hypoechoic solid	Absent	Smooth	Ovoid to round	Increased	-

Note.—+ = present.

- = absent.

FTC = follicular carcinoma, LN = lymph node, Lt = left, PTC = papillary carcinoma, Rt = right

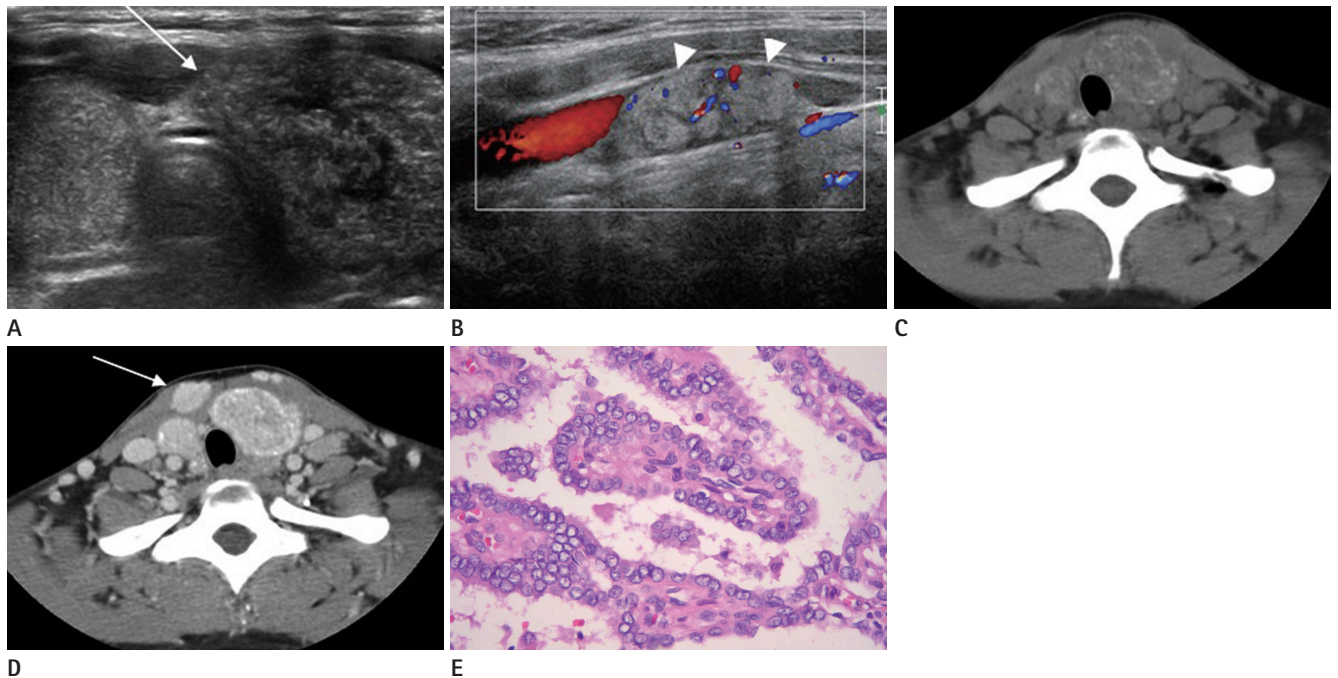


Fig. 2. A 13-year-old girl with papillary thyroid cancer.

Transverse **(A)** gray-scale US images depict goitrous enlargement with numerous microcalcifications (arrow), **(B)** metastatic lymph node with calcifications and hypervascularity (arrowheads).

The pre **(C)** and post **(D)** contrast-enhanced neck CT scan show diffuse heterogeneous enlargement of the thyroid gland with calcifications, a metastatic enhancing mass in the strap muscle, and both level IV nodes.

Histologic examination **(E)** shows classical papillary thyroid cancer with optically clear nuclei and nuclear pseudo-inclusions (H & E, $\times 400$).

DISCUSSION

Gender and age distribution in the present study were similar to those of other studies. Additionally, nine patients showed high T-staging; T3 ($n = 5$; 38.5%) and T4 ($n = 4$; 30.8%), and metastatic lymphadenopathy in the lateral neck ($n = 8$; 61.5%). These results are consistent with those of previous reports showing that pediatric thyroid cancer tends to present at a more advanced stage than that of adults (4). In a long term follow-up study reported by Zimmerman et al. (5), the incidence of distant metastasis was estimated to be 6.9% in children, with lymph node involvement in 89.7%.

PTC is the most common thyroid cancer in children; the prognosis is more favorable in young patients (7). In our study, the BRAF^{V600E} mutation was detected in three of ten patients (30.0%) with PTC which was a much lower frequency than what was found in Korean adults (70-83%) (12); however, it is higher than that of other reports on pediatric thyroid cancer (9). The BRAF^{V600E} mutation is intrinsically associated with increased progression and aggressiveness of PTC. Similarly, the BRAF^{V600E} mutation has a similarly high predictive value for PTC recurrence (11, 13). Pediatric PTC is highly curable and rarely recurs if treated with appropriate surgery with adjunctive radioiodine ablation, even if the initial disease is extensive and associated with extrathyroidal invasion, lymph node metastasis, or lung metastasis (19, 20). This is consistent

with the fact that the BRAF^{V600E} mutation rarely occurs in pediatric PTC (9, 10). In this small study population, we cannot explain the relevance of imaging findings in the prediction of prognosis. The low rate of the BRAF^{V600E} mutation in our study supports the concept that pediatric thyroid cancer is almost always differentiated and sensitive to radioiodine treatment, leading to a better prognosis.

Using gray-scale and power Doppler imaging, Lyshchik et al. (15) reported in their study of US features of thyroid cancer in children that only included focal nodular lesions of the thyroid. Although our study population was small, two out of nine patients (22.2%) showed US findings of diffuse enlargement with microcalcifications, which were confirmed to be classical PTC. The thyroid gland was replaced by tumor cells in these cases. Nodules were observed in patients who had underlying lymphocytic thyroiditis; one patient showed a typical malignant nodule, and the other, who presented with hyperthyroidism (thyroid uptake 7.2%; normal range 2-4%), showed an oval hyperechoic nodule with numerous microcalcifications. Thus, patients with a diffusely enlarged thyroid with microcalcifications should undergo FNA and BRAF^{V600E} analysis. Regarding nodules, US findings of nodules did not differ from malignant nodules in adults. All PTC nodules were suspicious malignant nodules according to the "Guidelines for the Thyroid US" by the Thyroid Study Group, Korean Society of Neuro- and Head and Neck Radiology. In the pres-

Table 3. Summary of CT Features in 12 Children and Adolescents with Thyroid Cancer

No.	Pathology	Attenuation*			Calcifications
		Pre-Contrast Enhancement	Post-Contrast Enhancement	Degree of Enhancement (%)	
1	PTC	Low	Heterogeneous, low	88.00	
2 [†]	PTC	Iso to low	Heterogeneous, low	132.35	+: micro
3	PTC	Low	Low	62.50	
4 [†]	PTC	Iso to low	Low	157.45	
5	PTC	Low	Heterogeneous, low	160.47	
6	PTC	Low	Heterogeneous, low	221.43	
7	PTC	Low	Low	80.36	
8	PTC	Low	Heterogeneous, low	Not taken	+: macro
9	PTC	Diffuse goitrous, heterogeneous, low	Heterogeneous, low	110.00	+: micro
10	PTC	Diffuse goitrous, heterogeneous, low	Heterogeneous, low	82.93	+: micro
11	FTC	Low	Iso	406.67	
12	FTC	Low	Heterogeneous, low	216.67	

Note.—*compared with to normal surrounding thyroid tissue.

[†]diffusely low attenuation of the thyroid gland, similar with to strap muscle on a precontrast scan due to underlying with lymphocytic thyroiditis; in these patients, attenuation of the nodules was compared with to the neck muscle.

FTC = follicular carcinoma, PTC = papillary carcinoma

ent study, calcifications (88.9%, 8/9) and intranodular vascularity (100%) on color Doppler images were frequent findings on US, whereas 33.3% (4/12) of the patients showed calcifications on CT scan. This difference was probably due to the fact that microcalcifications are more easily detected on US.

Because of the negative effect of postoperative I-131 ablation, the preoperative use of iodinated contrast agents in patients with thyroid cancer is discouraged (21). However, in the present study, contrast enhanced CT scans did not alter or affect patient management, because patients were required to wait until a therapeutic room for iodine ablation therapy became available. US can evaluate thyroid abnormalities and lymphadenopathy. CT scans are useful for the evaluation of lymph nodes at the level of VI or retropharyngeal nodes, which are limited areas on US. Furthermore, despite a very high accuracy of US according to a per patient analysis, the sensitivity of CT according to per level analysis is superior to that of US, so CT may play a complementary role in the determination of the surgical extent in selected patients with thyroid cancer (22). In our study, contrast-enhanced CT scans showed low attenuation nodular lesions in 11 patients (11/12) in comparison to well-enhanced surrounding thyroid glands. In one patient who underwent CT in an outside hospital, the degree of enhancement could not be calculated; the degree of enhancement ranged from 80 to 406% (mean, 166.9%) in 11 patients. Because this study included a small number of patients, a subsequent study comparing benign nodules in a larger group of patients will be required.

In summary, pediatric thyroid cancer tends to present with high T-stage. BRAF^{V600E} mutations were detected in 30.0% of cases, which is a lower frequency than the frequency found in adults. US features showed a goiterous enlargement with calcification ($n = 2$; 22.2%) or a nodular lesion ($n = 7$; 77.8%). We suggest that a diffusely enlarged thyroid with microcalcifications should be evaluated with FNA. On contrast-enhanced CT, a low attenuation nodule was the main finding.

REFERENCES

1. Khurana KK, Labrador E, Izquierdo R, Mesonero CE, Pisharodi LR. The role of fine-needle aspiration biopsy in the management of thyroid nodules in children, adolescents, and young adults: a multi-institutional study. *Thyroid* 1999;9:383-386
2. Collini P, Massimino M, Leite SF, Mattavelli F, Seregini E, Zucchini N, et al. Papillary thyroid carcinoma of childhood and adolescence: a 30-year experience at the Istituto Nazionale Tumori in Milan. *Pediatr Blood Cancer* 2006;46:300-306
3. Korea Central Cancer Registry Ministry of Health and Welfare Republic of Korea. 2002 Annual report of the Korea Central Cancer Registry. Seoul: Ministry of Health and Welfare Republic of Korea, 2003
4. Grigsby PW, Gal-or A, Michalski JM, Doherty GM. Childhood and adolescent thyroid carcinoma. *Cancer* 2002;95:724-729
5. Zimmerman D, Hay ID, Gough IR, Goellner JR, Ryan JJ, Grant CS, et al. Papillary thyroid carcinoma in children and adults: long-term follow-up of 1039 patients conservatively treated at one institution during three decades. *Surgery* 1988;104:1157-1166
6. Brink JS, van Heerden JA, McIver B, Salomao DR, Farley DR, Grant CS, et al. Papillary thyroid cancer with pulmonary metastases in children: long-term prognosis. *Surgery* 2000;128:881-886; discussion 886-887
7. Shapiro NL, Bhattacharyya N. Population-based outcomes for pediatric thyroid carcinoma. *Laryngoscope* 2005;115:337-340
8. Fenton CL, Lukes Y, Nicholson D, Dinanier CA, Francis GL, Tuttle RM. The ret/PTC mutations are common in sporadic papillary thyroid carcinoma of children and young adults. *J Clin Endocrinol Metab* 2000;85:1170-1175
9. Ciampi R, Nikiforov YE. RET/PTC rearrangements and BRAF mutations in thyroid tumorigenesis. *Endocrinology* 2007;148:936-941
10. Santoro M, Melillo RM, Fusco A. RET/PTC activation in papillary thyroid carcinoma: European Journal of Endocrinology Prize Lecture. *Eur J Endocrinol* 2006;155:645-653
11. Xing M. BRAF mutation in thyroid cancer. *Endocr Relat Cancer* 2005;12:245-262
12. Kim KH, Kang DW, Kim SH, Seong IO, Kang DY. Mutations of the BRAF gene in papillary thyroid carcinoma in a Korean population. *Yonsei Med J* 2004;45:818-821
13. Nikiforova MN, Kimura ET, Gandhi M, Biddinger PW, Knauf

- JA, Basolo F, et al. BRAF mutations in thyroid tumors are restricted to papillary carcinomas and anaplastic or poorly differentiated carcinomas arising from papillary carcinomas. *J Clin Endocrinol Metab* 2003;88:5399-5404
14. Bentley AA, Gillespie C, Malis D. Evaluation and management of a solitary thyroid nodule in a child. *Otolaryngol Clin North Am* 2003;36:117-128
15. Lyshchik A, Drozd V, Demidchik Y, Reiners C. Diagnosis of thyroid cancer in children: value of gray-scale and power doppler US. *Radiology* 2005;235:604-613
16. AJCC cancer staging Manual. 7th ed. Springer-Verlag, New York: Thyroid, 2010:87-96
17. Moon WJ. *Imaging Diagnosis*. In Thyroid Study group of Head and Neck society of Korean Radiology. *Thyroid gland: Imaging diagnosis and Intervention*. 1st ed. Seoul: Ilchokak, 2008:150-183
18. Recommended normative values for thyroid volume in children aged 6-15 years. World Health Organization & International Council for Control of Iodine Deficiency Disorders. *Bull World Health Organ* 1997;75:95-97
19. Demidchik YE, Demidchik EP, Reiners C, Biko J, Mine M, Saenko VA, et al. Comprehensive clinical assessment of 740 cases of surgically treated thyroid cancer in children of Belarus. *Ann Surg* 2006;243:525-532
20. Jarzab B, Handkiewicz-Junak D, Wloch J. Juvenile differentiated thyroid carcinoma and the role of radioiodine in its treatment: a qualitative review. *Endocr Relat Cancer* 2005;12:773-803
21. Nygaard B, Nygaard T, Jensen LI, Court-Payen M, S  e-Jensen P, Nielsen KG, et al. Iohexol: effects on uptake of radioactive iodine in the thyroid and on thyroid function. *Acad Radiol* 1998;5:409-414
22. Ahn JE, Lee JH, Yi JS, Shong YK, Hong SJ, Lee DH, et al. Diagnostic accuracy of CT and ultrasonography for evaluating metastatic cervical lymph nodes in patients with thyroid cancer. *World J Surg* 2008;32:1552-1558

소아와 청소년에서 갑상선암의 영상의학적 소견과 임상적 특징¹

이강영¹ · 홍현숙¹ · 이은혜¹ · 이범하¹ · 이해경¹ · 이용화² · 고은석³

목적: 소아 갑상선암의 임상적 특징, 영상소견, 유두상암종 환자의 BRAF^{V600E} 유전자 변이를 평가하였다.

대상과 방법: 13명의 소아 환자에서 BRAF^{V600E} 유전자 변이를 포함한 임상소견, 초음파 및 컴퓨터단층촬영(CT) 소견을 후향적으로 평가하였다. 초음파 소견은 병변의 위치, 결절의 유무, 에코결, 에코음영, 석회화, 경계, 모양, 결절 내 혈류, 비정상 림프절 등을 분석하였다. CT 스캔은 병변의 감식도, 석회화, 조영정도를 평가하였다.

결과: 3명의 남아와 10명의 여아를 대상으로 하였고 평균나이는 15.5세였다(연령분포, 6세~18세). 이전에 방사선에 노출된 환자는 없었다. 만저지는 경부 종괴가 가장 흔한 증상이었다. 조직 소견은 유두상암종이 11명, 여포상암종이 2명이었고 13명 중 9명은 높은 T 병기를 보였다. BRAF^{V600E} 변이는 유두상암종 환자 중 30%에서 발견되었다. 초음파 검사를 시행한 9명 중 7명은 결절의 형태로 보였고, 2명은 석회화를 동반한 미만성 갑상선 종대로 나타났다. 모든 유두상암종 결절은 악성 초음파 소견을 보였고 한 예의 여포상암종은 경계성 결절의 소견을 보였다. CT 스캔을 시행한 12명 중 11명이 조영증강 CT 스캔에서 저음영 결절의 형태를 보였다.

결론: 초음파 소견은 석회화를 동반한 미만성 종대 또는 결절의 소견을 보였다. 따라서 소아에서 갑상선의 미세석회화를 동반한 미만성 종대가 있을 경우 fine-needle aspiration을 시행하는 것이 필요하다고 생각된다. 조영증강 CT 스캔에서는 저음영 결절의 형태가 흔한 소견이었다.

순천향대학교 의과대학 부천병원 ¹영상의학과학교실, ²진단검사의학과학교실, ³병리과학교실